polymers

MDPI

Article

Biodegradable Shape Memory Polymeric Material from Epoxidized Soybean Oil and Polycaprolactone

Takashi Tsujimoto *, Takeshi Takayama and Hiroshi Uyama

Received: 28 September 2015 ; Accepted: 21 October 2015 ; Published: 27 October 2015
Academic Editor: Wei Min Huang

Department of Applied Chemistry, Graduate School of Engineering, Osaka University, Yamadaoka 2-1, Suita, Osaka 565-0871, Japan; t_takayama@chem.eng.osaka-u.ac.jp (T.T.); h_uyama@chem.eng.osaka-u.ac.jp (H.U.)
* Correspondence: tsujimoto@chem.eng.osaka-u.ac.jp; Tel.: +81-6-6879-7365; Fax: +81-6-6879-7367

Abstract: This article deals with the synthesis of plant oil-based shape memory materials from epoxidized soybean oil (ESO) and polycaprolactone (PCL). PolyESO/PCLs were synthesized by an acid-catalyzed curing in the presence of PCL. During the reaction, PCL scarcely reacted with ESO and the crystallinity of the PCL component decreased to form a semi-interpenetrating network structure. The incorporation of the PCL components improved the maximum stress and strain at break of ESO-based network polymer. The polyESO/PCL was gradually degraded by *Pseudomonas cepasia* lipase. Furthermore, the polyESO/PCLs exhibited excellent shape memory properties, and the strain fixity depended on the feed ratio of ESO and PCL. The shape memory-recovery behaviors were repeatedly practicable. The resulting materials are expected to contribute to the development of biodegradable intelligent materials.

Keywords: renewable resource; biodegradable; epoxidized soybean oil; shape memory polymer

1. Introduction

In recent years, a growing interest in the exploitation of renewable resources in the area of energy and materials has been one of the major scientific and industrial issues, because of the depletion of petroleum resources and economic considerations. Bio-based polymers and composites derived from renewable agricultural feedstock are a demonstrative case of a relevant dimension for sustainable development [1–3]. They have a large potential to substitute traditional petroleum-based products in the industry. Moreover, the advantages of these bio-based materials sometimes include composting and biodegradability after their use.

Among renewable resources, plant oils such as soybean oil, palm oil, linseed oil, and sunflower oil are expected as an ideal alternative chemical feedstock, since plant oils are found in abundance in the world [4]. Triglycerides are the major components in all plant oils, and these contain both saturated and unsaturated fatty acids. Inexpensive triglyceride plant oils have been utilized extensively for coatings, inks, plasticizers, lubricants, resins and agrochemicals, in addition to their applications in food industry. However, direct radical or cationic polymerization of most plant oils is structurally difficult due to their non-conjugated and internal double bonds, resulting in the formation of viscous liquid polymers with low molecular weight [5]. Due to these properties, when triglycerides have been a minor component in polymeric materials, they have been used solely as a modifier to improve their physical properties.

The most common modification of plant oils is the introduction of oxirane groups that replace double bonds in the unsaturated fatty acids. Epoxidized soybean oil (ESO), which is one of the most inexpensive vegetable oils in the world, is commercialized in large volumes at a reasonable cost. ESO is primarily used as a plasticizer for poly(vinyl chloride) to improve stability and flexibility.

The polyols and acrylates, which are converted from epoxidized plant oils, have been developed as starting materials for functional bio-based polymers [6–10]. Furthermore, the cationic polymerization of epoxidized plant oils has been investigated using photoinitiators, latent catalysts, and acid catalysts to produce bio-based epoxy resins. Although these epoxy compounds from renewable resources possess a high potential as a starting material for bio-based thermosetting plastics, the triglycerides are made up of aliphatic chains, and consequently, the plant oil-based materials are incapable of the rigidity and strength required for some applications by themselves [11–15]. ESO was cured in the presence of inorganic chemicals to produce organic-inorganic hybrid materials [16–19]. Plant oil-based green composites were developed using biofibers such as kenaf, flax, hemp, and rosin derivatives as renewable compounds to improve their poor mechanical properties [20–23].

Shape memory materials are one of the early-developing and emerging smart materials. Shape memory materials change their shapes reversibly from temporary to permanent by mechanical loading and external stimulus, which may be temperature, light, pH, humidity, chemical, and electricity [24–30]. Because of their good processability, low cost, and high recovery ability, shape memory polymers have received much attention and have been used in various fields, with applications such as sensors, transducers, actuators, and medical implants. The thermally-triggered shape memory polymer is first processed to receive a permanent shape. The temporary shape is set by deformation above a certain transition temperature (switching temperature) and subsequent cooling under loading. This process typically relies on vitrification, crystallization, and other physical interactions such as hydrogen bonding and ionic bonding. When reheated above the switching temperature without loading, the oriented polymer chains are released, resulting in a macroscopic recovery of the original shape. Up to now, numerous polymers, including polyurethane, polynorbornene, *trans*-polyisoprene, and styrene-butadiene copolymer, have been found to have attractive shape memory effects [31–38]. Bio-based shape memory polymers have also been developed from glycerol, glycolide, and lactide [39–44]. Several researchers exploited polycaprolactone (PCL)-based shape memory polymers, and these materials showed sharper and faster shape memory-recovery behaviors by using melting/recrystallization of the PCL component as a switching transition [45–47]. However, most of them are block copolymers that were prepared by means of a two-stage synthesis or coupling method.

In this study, we synthesized a biodegradable polymeric material with semi-interpenetrating network structure from epoxidized soybean oil and polycaprolactone, and measured the thermal and mechanical properties. Furthermore, the shape memory properties of the resulting material were investigated.

2. Experimental Section

2.1. Materials

ESO and a thermally-latent cationic catalyst (benzylsulfonium hexafluoroantimonate derivative, Sun-Aid SI-100L) were gifts from Adeka Co. (Tokyo, Japan) and Sanshin Chemical Industry Co. (Yamaguchi, Japan), respectively. Polycaprolactone (PCL) (M_n = 8.0 × 10^4) was purchased from Sigma-Aldrich Co. (St. Louis, MO, USA). Other reagents and solvents were commercially available and were used as received.

2.2. Synthesis of PolyESO/PCL

The synthesis of polyESO/PCL was carried out as follows. ESO (0.5 g) and PCL (0.5 g) were dissolved in 2.5 mL of chloroform, and a thermally-latent cationic catalyst was added to the solution. The solution was poured into a Teflon mold (17 mm × 40 mm × 1 mm), and then, the solvent was allowed to evaporate at room temperature. The residual mixture was kept at 150 °C for 2 h to produce polyESO/PCL (50/50 wt %).

The polyESO/PCLs with different feed ratios of ESO and PCL were prepared by a similar procedure.

2.3. Enzymatic Degradation of PolyESO/PCL

The polyESO/PCL (50/50 wt %) with dimensions of 10 mm × 10 mm was placed in a vial containing 20 mL of phosphate buffer (pH 7.2) and 10 mg of lipase from *Pseudomonas cepacia*, and the vial was shaken gently. At the predetermined degradation time, the sample was removed from the buffer, washed with deionized water, and dried *in vacuo* for 24 h. The degradation test was performed three times. The weight of the residue was measured to evaluate the degree of degradation.

2.4. Evaluation of Shape Memory-Recovery Properties of PolyESO/PCL

Shape memory-recovery properties were evaluated by the end-to-end length of the sample to determine the strain fixity and the shape recovery. The polyESO/PCL with a rectangular bar (sample length: L) was prepared as a permanent shape. The sample was heated at 80 °C and loaded to the predetermined strain, followed by cooling and unloading at 20 °C. Upon unloading, a part of the strain was instantaneously recovered, leaving an unloading strain (ε_u). Then, the sample was reheated at 80 °C to recover the strain, leaving a recovery strain (ε_r). The strain fixity and the shape recovery are defined as follows.

$$\text{Strain fixity}\,(\%) = (L - \varepsilon_u)/L \times 100 \quad (1)$$

$$\text{Recovery}\,(\%) = \varepsilon_r/L \times 100 \quad (2)$$

2.5. Measurements

^{1}H nuclear magnetic resonance (^{1}H NMR) spectrum was measured by a DPX-400 instrument (Bruker Biospin Co., Billerica, MA, USA). Fourier-transform infrared spectroscopy (FT-IR) was recorded on a Spectrum One (Perkin-Elmer Inc., Waltham, MA, USA). The thermal properties of the samples were investigated under nitrogen atmosphere by using a DSC6020 differential scanning calorimeter (DSC) (Hitachi High-Tech Science Co., Tokyo, Japan). The sample was heated from −100 to 180 °C at a heating rate of 10 °C·min^{-1}, and the temperature was maintained for a duration of 3 min. Then, the sample was cooled to −100 °C at a cooling rate of 10 °C·min^{-1}. The temperature was maintained for a duration of 3 min, and the sample was reheated to 200 °C at a heating rate of 10 °C·min^{-1}. Tensile properties were measured by using a EZ Graph (Shimadzu Co., Kyoto, Japan) with a cross-head speed of 5 mm·min^{-1}. The sample was cut into a plate shape of 5 mm × 20 mm ×1 mm. Wide-angle X-ray scattering (WAXS) analysis was performed using RINT2500 instrument (Rigaku Co., Tokyo, Japan) with CuKα radiation at 50 kV/300 mA. The diffractogram was scanned in a 2θ range of 1.5°–40° at a rate of 2°·min^{-1}. Dynamic viscoelasticity analysis (DMA) was performed by using a DMS6100 (Hitachi High-Tech Science Co., Tokyo, Japan) with a frequency of 1 Hz at a heating rate of 3 °C·min^{-1}.

3. Results and Discussion

3.1. Synthesis of PolyESO/PCL

In this study, epoxidized soybean oil (ESO) was used as an epoxide monomer. The oxirane group number of ESO, determined by ^{1}H NMR spectroscopy, was 3.7 per molecule. The polyESO/PCLs were synthesized by the curing of ESO using a thermally-latent cationic catalyst in the presence of PCL at 150 °C to produce flexible pale brown materials (Figure 1). In the FT-IR spectrum of the polyESO/PCL, a peak at *ca.* 820 cm^{-1} ascribed to C–C anti-symmetric stretching of the oxirane groups of ESO disappeared. On the other hand, the peaks ascribed to C=O stretching of carbonyl groups of the ESO and PCL hardly changed (Figure S1, Supplementary Materials). The polyESO/PCLs

were immersed in chloroform at room temperature for 24 h, and the residue was washed with chloroform. The PCL components were dissolved in chloroform, and the residue weight was close to the feed weight of ESO. These results indicate that the PCL component is scarcely reacted during the crosslinking of ESO to form a semi-interpenetrating polymer network structure.

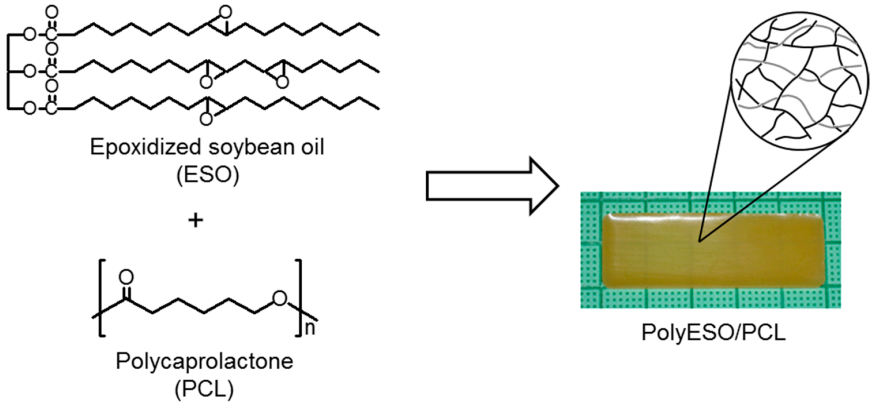

Figure 1. Synthesis of polyESO/PCL.

3.2. Thermal and Mechanical Properties of polyESO/PCL

In order to investigate the thermal properties of the polyESO/PCL, DSC measurement of the ESO homopolymer, the polyESO/PCLs, and neat PCL was carried out (Figure 2). In the DSC curve of the ESO homopolymer, a glass transition was observed at −25 °C. On the other hand, the curve of neat PCL showed a glass transition and a melting behavior at −63 and 59 °C, respectively. In the curves of the polyESO/PCLs, glass transitions of ESO polymer and PCL were not observed, and the melting temperature (T_m) of the PCL component decreased with an increase in the ESO content. Moreover, the melting enthalpy (ΔH_m) per 1 g of PCL also decreased compared with that of neat PCL. These results may indicate that PCL components are partly miscible with the ESO polymer. Both curves of the ESO homopolymer and the polyESO/PCLs were almost constant in the higher temperature region, suggesting the quantitative consumption of the oxirane groups of ESO.

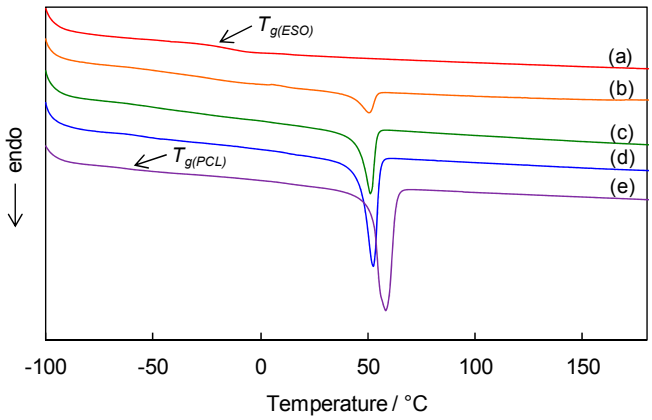

Figure 2. Differential Scanning Calorimetry (DSC) curves of second heating scan for (**a**) ESO homopolymer; (**b**) polyESO/PCL (75/25 wt %); (**c**) polyESO/PCL (50/50 wt %); (**d**) polyESO/PCL (25/75 wt %); and (**e**) neat PCL.

The thermal and mechanical properties such as melting temperature, melting enthalpy, maximum stress, and strain at break, are summarized in Table 1. In the tensile test, neat PCL showed ductile behavior. Following the yield point, neat PCL could be stretched further, followed

up by strain hardening to an elongation of 1000% which is the maximum extension limit of our instrument. On the other hand, the ESO homopolymer was brittle and fractured at low strain, due to the ESO-based network structure. The maximum stress of the polyESO/PCLs increased as the PCL content increased. Moreover, the strain at break of the polyESO/PCLs was larger than that of the ESO homopolymer. This may be because the incorporation of PCL components increased the distance between crosslinking points of ESO-based network polymer.

Table 1. Thermal and mechanical properties of polyESO/PCL.

Sample code	T_m [a]	ΔH_m [a,b]	Maximum stress [c]	Strain at break [c]
	°C	J·g^{-1}	MPa	%
ESO homopolymer	– [d]	– [d]	1.0	9
PolyESO/PCL (75/25 wt %)	50.6	9.8	2.6	20
PolyESO/PCL (50/50 wt %)	51.6	25.7	8.8	63
PolyESO/PCL (25/75 wt %)	52.8	41.6	12.3	147
Neat PCL	58.6	62.2	– [e]	>1,000

[a] Determined by DSC; [b] Melting enthalpy of whole sample; [c] Determined by tensile test; [d] Not observed; [e] Not measured. Melting temperature (T_m); Melting enthalpy (ΔH_m).

In order to investigate the microstructure of the PCL component in polyESO/PCL, wide-angle X-ray diffraction (WAXD) was measured (Figure 3). It is found that the microstructure of the polyESO/PCL (50/50 wt %) is characterized by superposition of an amorphous halo and crystalline diffraction peaks of 2θ = 21.5°, 22.0°, and 23.7° that correspond to the (010), (111) and (112) planes of PCL crystal [48]. These suggest that the microstructure of the PCL component in polyESO/PCL is not changed compared to neat PCL except for a decrease of crystallinity.

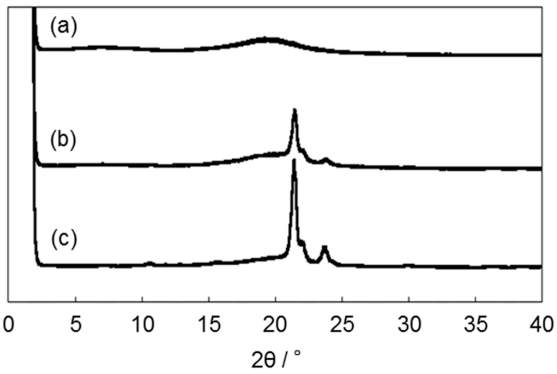

Figure 3. X-ray diffraction patterns of (**a**) ESO homopolymer; (**b**) polyESO/PCL (50/50 wt %); and (**c**) neat PCL.

Figure 4 shows the dynamic viscoelasticity (storage modulus and loss factor) as a function of temperature for the ESO homopolymer, the polyESO/PCLs and neat PCL. For all samples, the storage moduli remained almost constant between −100 and −70 °C, and decreased as temperature increased. In the ESO homopolymer, the rapid decrease of the storage modulus was observed at −25 °C. At higher temperatures, the storage modulus of the ESO homopolymer was almost constant, indicating the quantitative consumption of oxirane groups and the formation of a plant oil-based network polymer. The storage modulus of neat PCL slightly decreased at −70 °C due to the glass transition of PCL, and PCL melted at *ca.* 50 °C. It is found that the storage moduli of polyESO/PCLs drop stepwise. At lower temperature, the polyESO/PCLs were glassy with a storage modulus more than 1.0 GPa. The storage modulus of the polyESO/PCLs gradually decreased from −60 to 0 °C, resulting in the first rubbery state. With an increase in the ESO content, the storage modulus in first

rubbery state decreased. Only a broad peak was found in loss factor curves of the polyESO/PCLs, and the peaks shifted to the higher temperature region as the ESO content increased. These indicate that the PCL components are partly miscible with the ESO polymer in polyESO/PCLs. Upon further heating, the storage modulus dropped at *ca.* 50 °C, which was derived from the melting temperature of PCL, to give the second rubbery state. These results are in good agreement with DSC analysis. In the second rubbery region, the storage moduli of polyESO/PCLs were constant due to the plant oil-based network structure and the polyESO/PCLs with the ESO content of 50 and 75 wt % exhibited a relatively high storage modulus of more than 1.0 MPa. The storage modulus in the second rubbery region depended on the ESO content. In shape memory polymers, the storage modulus below the switching temperature governs the strength of the materials, whereas the modulus above the switching temperature determines the recovery force. In this study, the transition between the first rubbery state and the second rubbery state was used as a switching transition of shape memory-recovery behaviors.

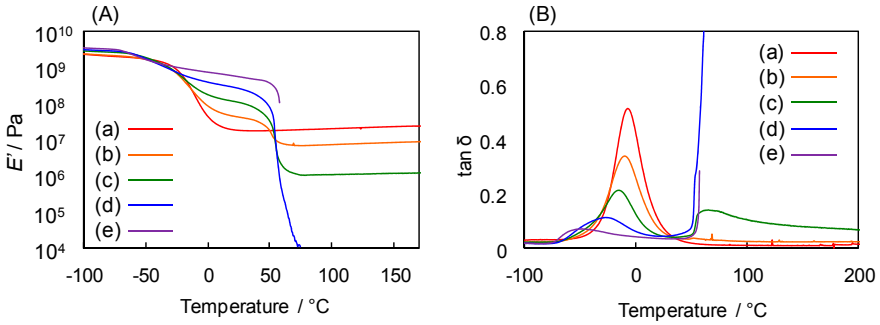

Figure 4. Dynamic viscoelasticity of (a) ESO homopolymer, (b) polyESO/PCL (75/25 wt %), (c) polyESO/PCL (50/50 wt %), (d) polyESO/PCL (25/75 wt %), and (e) neat PCL; (**A**) storage modulus, and (**B**) loss factor.

PCL is one of the most promising synthetic polymers that can degrade in contact with enzymes and microorganisms. PCL is also a biocompatible and nontoxic polyester, like poly(lactic acid) and polyglycoside. Enzymatic degradation of the polyESO/PCL (50/50 wt %) was performed using lipase from *Pseudomonas cepasia*. The enzymatic hydrolysis gradually took place, and biodegradability reached 40% at 5 days (Figure 5). The loss weight was close to the feed weight of PCL. On the other hand, the weight of the ESO homopolymer hardly changed, suggesting that the lipase from *Pseudomonas cepasia* degraded the PCL components. In our previous study, an ESO-based network polymer could be degraded in activated sludge [16]. Therefore, the resulting polyESO/PCLs exhibited high potential for biodegradable materials.

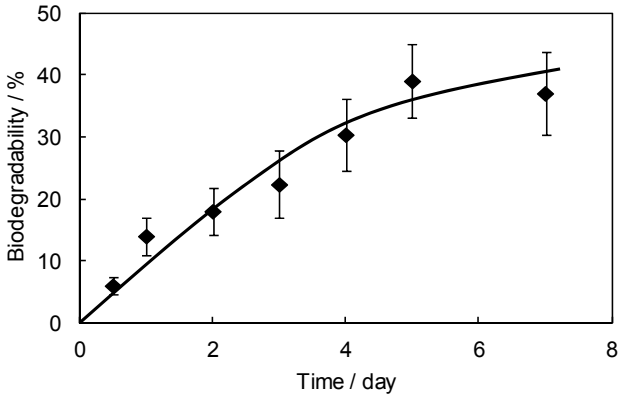

Figure 5. Enzymatic hydrolysis behavior of polyESO/PCL (50/50 wt%).

3.3. Shape Memory-Recovery Behavior of PolyESO/PCL

An investigation of shape memory-recovery behaviors of the polyESO/PCLs was performed. In this study, the melting/recrystallization of the PCL component was used as a switching transition of shape memory-recovery effect. A typical example of shape memory-recovery behaviors of the polyESO/PCL (50/50 wt %) is shown in Figure 6. During the crosslinking process, the primary shape without stress (permanent shape) was set to be a spiral shape. Above the melting temperature of the PCL component, the crystal of PCL melted, and the polyESO/PCL (50/50 wt %) was deformed into a rectangular bar (temporary shape). The subsequent cooling at room temperature fixed the deformed shape. Upon reheating above the melting temperature of the PCL component, the temporary shape was restored to its original shape. The recovery time was dependent on the operating temperature and feed ratio of ESO and PCL, and the permanent shape of polyESO/PCL (50/50 wt %) was recovered at 80 °C after 25 s. These deformations and recovery processes were repeatedly practicable. The plausible shape memory-recovery mechanism is as follows. The crystal of PCL fixes the shape of the sample and the driving force of shape recovery process is the elastic force of the ESO-based network polymer, generated during deformation. Above the switching temperature, PCL components in the polyESO/PCLs melt and the sample is easily deformed. After the subsequent cooling, the melt crystallization of PCL components proceeds, and the temporary shape is fixed with the internal stress of the ESO-based network polymer. Upon reheating above the melting temperature of PCL, the mobility of polymer chains increases, and the shape of the sample returns to the original shape by the entropy elasticity of the ESO-based network polymer.

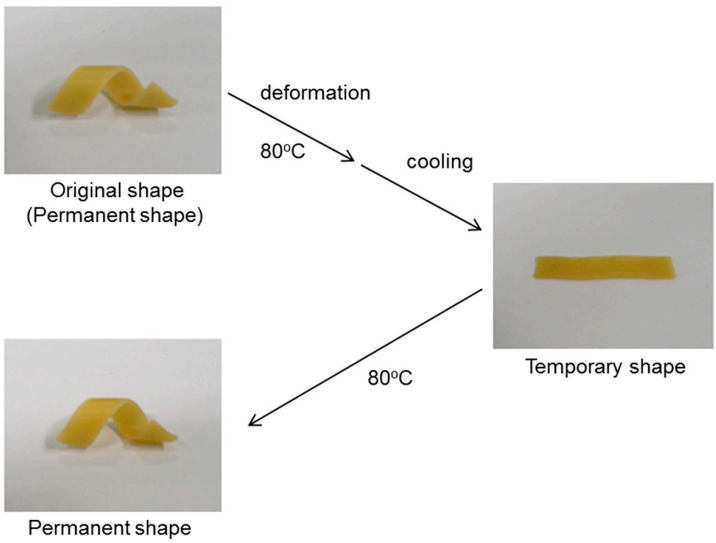

Figure 6. Shape memory-recovery behaviors of polyESO/PCL (50/50 wt %).

To investigate the ability of shape memory-recovery properties, we prepared the polyESO/PCLs with a rectangular bar as a permanent shape. The sample was deformed to a circle shape as a temporary shape (Figure S2, Supplementary Materials), and the strain fixity and recovery were evaluated by end-to-end length of the sample (Figure 7). The ESO homopolymer could not be deformed because of the brittleness, and the temporary shape of neat PCL was not prepared due to melting. All of the polyESO/PCLs showed good recovery ability. The strain fixity of the polyESO/PCL (75/25 wt %) decreased compared with that of the polyESO/PCL (50/50 wt %) and the polyESO/PCL (25/75 wt %), due to the decrease of the crystallinity of the PCL component and the increase of internal stress of the ESO-based polymer network. These results indicate that the shape recovery from the deformed shape to the original shape is attributed to the relaxation of the inner stress of the ESO-based polymer network. Furthermore, even at the fifth cycle, the strain fixity and

the recovery of the polyESO/PCL (50/50 wt %) and polyESO/PCL (25/75 wt %) were more than 90%, suggesting good reusability.

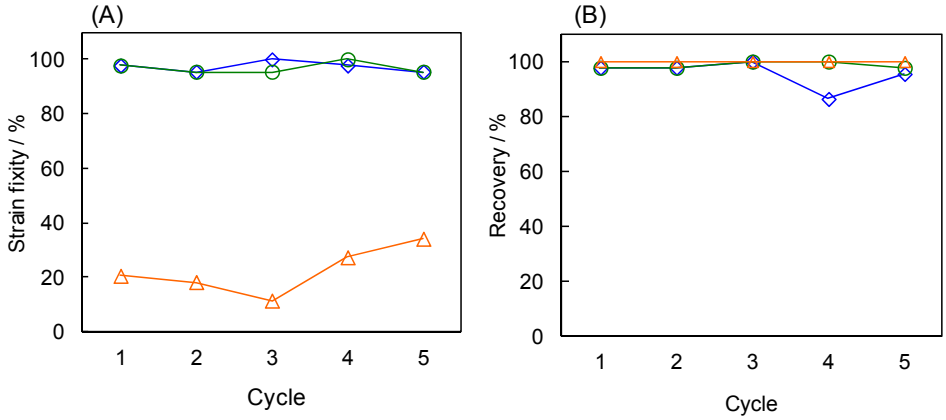

Figure 7. Shape memory-recovery properties of (Δ) polyESO/PCL (75/25 wt %), (◯) polyESO/PCL (50/50 wt %), and (◇) polyESO/PCL (25/75 wt %); (**A**) strain fixity, and (**B**) recovery.

4. Conclusions

In this study, a plant oil-based shape memory material was synthesized from epoxidized soybean oil and PCL. An acid-catalyzed crosslinking of ESO in the presence of PCL produced a flexible material with a semi-interpenetrating network structure. In the resulting polyESO/PCLs, PCL components were partly miscible with the ESO polymer, and the crystallinity of PCL components decreased. The mechanical properties, such as maximum stress and strain at break, were effectively improved by the incorporation of the PCL components. The PCL components in the polyESO/PCL were gradually hydrolyzed by lipase from *Pseudomonas cepasia*. Furthermore, the polyESO/PCLs exhibited excellent shape memory-recovery behaviors. The strain fixity was dependent on the feed ratio of ESO and PCL, and the deformation and recovery processes of the polyESO/PCLs were repeatedly practicable. These striking results provide a new strategy for designing novel biodegradable smart materials.

Supplementary Materials: The supplementary materials is available online at: www.mdpi.com/2073-4360/7/10/1506/s1.

Acknowledgements: This study was supported by a Grant-in-Aid for Young Scientists from Japan Society for the Promotion of Science (JSPS) (No. 268101140).

Author Contributions: In this study, Takashi Tsujimoto and Hiroshi Uyama designed the experiments and involved in all data analysis. Takashi Tsujimoto and Takeshi Takayama performed the experiments and collected data. Takashi Tsujimoto wrote the paper.

Conflicts of Interest: The authors declare no conflict of interest.

References

1. Ragauskas, A.J.; Williams, C.K.; Davison, B.H.; Britovsek, G.; Cairney, J.; Eckert, C.A.; Frederick, W.J., Jr.; Hallett, J.P.; Leak, D.J.; Liotta, C.L.; *et al*. The path forward for biofuels and biomaterials. *Science* **2006**, *311*, 484–489. [CrossRef] [PubMed]
2. Nagarajan, V.; Mohanty, A.K.; Misra, M. Sustainable green composites: Value addition to agricultural residues and perennial grasses. *ACS Sustain. Chem. Eng.* **2013**, *1*, 325–333. [CrossRef]
3. Quirino, R.L.; Garrison, T.F.; Kessler, M.R. Matrices from vegetable oils, cashew nut shell liquid, and other relevant systems for biocomposite applications. *Green Chem.* **2014**, *16*, 1700–1715. [CrossRef]
4. Biermann, U.; Friedt, W.; Lang, S.; Lühs, W.; Machmüller, G.; Metzger, J.O.; Rüsch gen Klaas, M.; Schäfer, H.J.; Schneider, M.P. New syntheses with oils and fats as renewable raw materials for the chemical industry. *Angew. Chem. Int. Ed.* **2000**, *39*, 2206–2224. [CrossRef]

5. Petrović, Z.S. Polyurethanes from vegetable oils. *Polym. Rev.* **2008**, *48*, 109–155. [CrossRef]
6. Swern, D.; Billen, G.N.; Findley, T.W.; Scanlan, J.T. Hydroxylation of monounsaturated fatty materials with hydrogen peroxide. *J. Am. Chem. Soc.* **1945**, *67*, 1786–1789. [CrossRef]
7. Lu, J.; Khot, S.; Wool, R.P. New sheet molding compound resins from soybean oil. I. Synthesis and characterization. *Polymer* **2005**, *46*, 71–80. [CrossRef]
8. Lligadas, G.; Ronda, J.C.; Galià, M.; Cádiz, V. Plant oils as platform chemicals for polyurethane synthesis: Current state-of-the-art. *Biomacromolecules* **2010**, *11*, 2825–2835. [CrossRef] [PubMed]
9. Luo, Q.; Liu, M.; Xu, Y.; Ionescu, M.; Petrović, Z.S. Thermosetting allyl resins derived from soybean oil. *Macromolecules* **2011**, *11*, 7149–7157. [CrossRef]
10. Saithai, P.; Lecomte, J.; Dubreucq, E.; Tanrattanakul, V. Effects of different epoxidation methods of soybean oil on the characteristics of acrylated epoxidized soybean oil-*co*-poly(methyl methacrylate) copolymer. *Express Polym. Lett.* **2013**, *7*, 910–924. [CrossRef]
11. Chakrapani, S.; Crivello, J.V. Synthesis and photoinitiated cationic polymerization of epoxidized castor oil and its derivatives. *J. Macromol. Sci. Pure Appl. Chem.* **1998**, *35*, 1–20. [CrossRef]
12. Biresaw, G.; Liu, Z.S.; Erhan, S.Z. Investigation of the surface properties of polymeric soaps obtained by ring-opening polymerization of epoxidized soybean oil. *J. Appl. Polym. Sci.* **2008**, *108*, 1976–1985. [CrossRef]
13. Gupta, A.P.; Ahmad, S.; Dev, A. Modification of novel bio-based resin-epoxidized soybean oil by conventional epoxy resin. *Polym. Eng. Sci.* **2011**, *51*, 1087–1091. [CrossRef]
14. Wang, R.; Schuman, T.P. Vegetable oil-derived epoxy monomers and polymer blends: A comparative study with review. *Express Polym. Lett.* **2013**, *7*, 272–292. [CrossRef]
15. Hosoda, N.; Tsujimoto, T.; Uyama, H. Plant oil-based green composite using porous poly(3-hydroxybutyrate). *Polym. J.* **2014**, *46*, 301–306. [CrossRef]
16. Tsujimoto, T.; Uyama, H.; Kobayashi, S. Green nanocomposites from renewable resources: Biodegradable plant oil-silica hybrid coatings. *Macromol. Rapid Commun.* **2003**, *24*, 711–714. [CrossRef]
17. Miyagawa, H.; Misra, M.; Drazal, L.T.; Mohanty, A.K. Novel biobased nanocomposites from functionalized vegetable oil and organically-modified layered silicate clay. *Polymer* **2005**, *46*, 445–453. [CrossRef]
18. Lligadas, G.; Ronda, J.C.; Galià, M.; Cádiz, V. Bionanocomposites from renewable resources: Epoxidized linseed oil-polyhedral oligomeric silsesquioxanes hybrid materials. *Biomacromolecules* **2006**, *7*, 3521–3526. [CrossRef] [PubMed]
19. Tanrattanakul, V.; Saithai, P. Mechanical properties of bioplastics and bioplastic-organoclay nanocomposites prepared from epoxidized soybean oil with different epoxide contents. *J. Appl. Polym. Sci.* **2009**, *114*, 3057–3067. [CrossRef]
20. Williams, G.I.; Wool, R.P. Composites from natural fibers and soy oil resins. *Appl. Compos. Mater.* **2000**, *7*, 421–432. [CrossRef]
21. Rakotonirainy, A.M.; Padua, G.W. Effects of lamination and coating with drying oils on tensile and barrier properties of zein films. *J. Agric. Food Chem.* **2001**, *49*, 2860–2863. [CrossRef] [PubMed]
22. Tran, P.; Graiver, D.; Narayan, R. Biocomposites synthesized from chemically modified soy oil and biofibers. *J. Appl. Polym. Sci.* **2006**, *102*, 69–75. [CrossRef]
23. Shibata, M.; Teramoto, N.; Someya, Y.; Suzuki, S. Bio-based nanocomposites composed of photo-cured epoxidized soybean oil and supramolecular hydroxystearic acid nanofibers. *J. Polym. Sci. Polym. Phys.* **2009**, *47*, 669–673. [CrossRef]
24. Feninat, F.E.; Laroche, G.; Fiset, M.; Mantovani, D. Shape memory materials for biomedical applications. *Adv. Eng. Mater.* **2002**, *4*, 91–104. [CrossRef]
25. Liu, C.; Seung, B.C.; Mather, P.T.; Zheng, L.; Haley, E.H.H.; Coughlin, E.B. Chemically cross-linked polycyclooctene: Synthesis, characterization, and shape memory behavior. *Macromolecules* **2002**, *35*, 9868–9874. [CrossRef]
26. Kolesov, I.S.; Radusch, H.J. Multiple shape-memory behavior and thermal-mechanical properties of peroxide cross-linked blends of linear and short-chain branched polyethylenes. *Express Polym. Lett.* **2008**, *2*, 461–473. [CrossRef]
27. Luo, X.; Mather, P.T. Triple-shape polymeric composites (TSPCs). *Adv. Funct. Mater.* **2010**, *20*, 2649–2656. [CrossRef]
28. Ranta, D.; Karger-Kocsis, J. Shape memory polymer system of semi-interpenetrating network structure composed of crosslinked poly(methyl methacrylate) and poly(ethylene oxide). *Polymer* **2011**, *52*, 1063–1070.

29. Julich-Gruner, K.K.; Löwenberg, C.; Neffe, A.T.; Behl, M.; Lendlein, A. Recent advances in polymer shape memory. *Macromol. Chem. Phys.* **2013**, *214*, 527–536. [CrossRef]
30. Fejős, M.; Molnár, K.; Karger-Kocsis, J. Epoxy/polycaprolactone systems with triple-shape memory effect: Electrospun nanoweb with and without graphene *versus* co-continuous morphology. *Materials* **2013**, *6*, 4489–4504. [CrossRef]
31. Alteheld, A.; Feng, Y.K.; Kelch, S.; Lendlein, A. Biodegradable, amorphous copolyester-urethane networks having shape-memory properties. *Angew. Chem. Int. Ed.* **2005**, *44*, 1188–1192. [CrossRef] [PubMed]
32. Ni, X.Y.; Sun, X.H. Block copolymer of *trans*-polyisoprene and urethane segment: Shape memory effects. *J. Appl. Polym. Sci.* **2006**, *100*, 879–885. [CrossRef]
33. Xue, L.; Dai, S.Y.; Li, Z. Synthesis and characterization of three-arm poly(ε-caprolactone)-based poly(ester-urethanes) with shape-memory effect at body temperature. *Macromolecules* **2009**, *42*, 964–972. [CrossRef]
34. Zhang, H.; Wang, H.; Zhong, W.; Du, Q. A novel type of shape memory polymer blend and the shape memory mechanism. *Polymer* **2009**, *50*, 1596–1601. [CrossRef]
35. Yang, D.; Gao, D.; Zeng, C.; Jiang, J.; Xie, M. POSS-enhanced shape-memory copolymer of polynorbornene derivate and polycyclooctene through ring-opening metathesis polymerization. *React. Funct. Polymers* **2011**, *71*, 1096–1101. [CrossRef]
36. Lu, H.B.; Huang, W.M.; Yao, Y.T. Review of chemo-responsive shape change/memory polymers. *Pigment Resin Technol.* **2013**, *42*, 237–246. [CrossRef]
37. Wu, X.L.; Huang, W.M.; Tan, H.X. Characterization of shape recovery via creeping and shape memory effect in ether-vinyl acetate copolymer (EVA). *J. Polym. Res.* **2013**, *20*, 150. [CrossRef]
38. Tsujimoto, T.; Toshimitsu, K.; Uyama, H.; Takeno, S.; Nakazawa, Y. Maleated *trans*-1,4-polyisoprene from *Eucommia ulmodies* oliver with dynamic network structure and its shape memory property. *Polymer* **2014**, *55*, 6488–6493. [CrossRef]
39. Takahashi, T.; Hayashi, N.; Hayashi, S. Structure and properties of shape-memory polyurethane block copolymers. *J. Appl. Polym. Sci.* **1996**, *60*, 1061–1069. [CrossRef]
40. Zini, E.; Scandola, M. Shape memory behavior of novel (L-lactide-glycolide-trimethylene carbonate) terpolymers. *Biomacromolecules* **2007**, *8*, 3661–3667. [CrossRef] [PubMed]
41. Cai, W.; Liu, L.L. Shape-memory effect of poly (glycerol-sebacate) elastomer. *Mater. Lett.* **2008**, *62*, 2171–2173. [CrossRef]
42. Yamashiro, M.; Inoue, K.; Iji, M. Recyclable shape-memory and mechanical strength of poly(lactic acid) compounds cross-linked by thermo-reversible Diels-Alder reaction. *Polym. J.* **2008**, *40*, 657–662. [CrossRef]
43. Guo, B.; Chen, Y.; Lei, Y.; Zhang, L.; Zhou, W.Y.; Bakr, A.; Rabie, M.; Zhao, J. Biobased poly(propylene sebacate) as shape memory polymer with tunable switching temperature for potential biomedical applications. *Biomacromolecules* **2011**, *12*, 1312–1321. [CrossRef] [PubMed]
44. Tsujimoto, T.; Uyama, H. Full bio-based polymeric material from plant oil and poly(lactic acid) with a shape memory property. *ACS Sustain. Chem. Eng.* **2014**, *2*, 2057–2062. [CrossRef]
45. Xu, X.L.; Sun, Z.J.; Cai, W.; Guo, Z.Y. Study on the shape memory effects of poly(L-lactide-*co*-ε-caprolactone) biodegradable polymers. *J. Mater. Sci. Mater. Med.* **2008**, *19*, 395–399.
46. Paderni, K.; Pandini, S.; Passera, S.; Pilati, F.; Toselli, M.; Messori, M. Shape-memory polymer networks from sol-gel cross-linked alkoxysilane-terminated poly(ε-caprolactone). *J. Mater. Sci.* **2012**, *47*, 4354–4362. [CrossRef]
47. Pandini, S.; Baldi, F.; Paderni, K.; Messori, M.; Toselli, M.; Pilati, F.; Gianoncelli, A.; Brisotto, M.; Brontempi, E.; Riccò, T. One-way and two-way shape memory behavior of semi-crystalline networks based on sol-gel cross-linked poly(ε-caprolactone). *Polymer* **2013**, *54*, 4253–4265. [CrossRef]
48. Hu, H.; Dorset, D.L. Crystal structure of poly(ε-capro1actone). *Macromolecules* **1990**, *23*, 4604–4607. [CrossRef]